JMolMed

ORIGINAL ARTICLE

Large extracellular vesicles derived from human regulatory macrophages (L-EV$_{Mreg}$) attenuate CD3/CD28-induced T-cell activation in vitro

Martin Albrecht[1] · Lars Hummitzsch[1] · Rene Rusch[2] · Christine Eimer[1] · Melanie Rusch[2] · Katharina Heß[3] ·
Markus Steinfath[1] · Jochen Cremer[2] · Fred Fändrich[4] · Rouven Berndt[2] · Karina Zitta[1]

Abstract

Macrophages belong to the innate immune system, and we have recently shown that in vitro differentiated human regulatory macrophages (Mreg) release large extracellular vesicles (L-EV$_{Mreg}$) with an average size of 7.5 μm which regulate wound healing and angiogenesis in vitro. The aim of this study was to investigate whether L-EV$_{Mreg}$ also affect the CD3/CD28-mediated activation of T-cells. Mreg were differentiated using blood monocytes and L-EV$_{Mreg}$ were isolated from culture supernatants by differential centrifugation. Activation of human T-cells was induced by CD3/CD28-coated beads in the absence or presence of Mreg or different concentrations of L-EV$_{Mreg}$. Inhibition of T-cell activation was quantified by flow cytometry and antibodies directed against the T-cell marker granzyme B. Phosphatidylserine (PS) exposure on the surface of Mreg and L-EV$_{Mreg}$ was analyzed by fluorescence microscopy. Incubation of human lymphocytes with CD3/CD28 beads resulted in an increase of cell size, cell granularity, and number of granzyme B–positive cells ($P < 0.05$) which is indicative of T-cell activation. The presence of Mreg (0.5×10^6 Mreg/ml) led to a reduction of T-cell activation (number of granzyme B–positive cells; $P < 0.001$), and a similar but less pronounced effect was also observed when incubating activated T-cells with L-EV$_{Mreg}$ ($P < 0.05$ for 3.2×10^6 L-EV$_{Mreg}$/ml). A differential analysis of the effects of Mreg and L-EV$_{Mreg}$ on CD4$^+$ and CD8$^+$ T-cells showed an inhibition of CD4$^+$ T-cells by Mreg ($P < 0.01$) and L-EV$_{Mreg}$ ($P < 0.05$ for 1.6×10^6 L-EV$_{Mreg}$/ml; $P < 0.01$ for 3.2×10^6 L-EV$_{Mreg}$/ml). A moderate inhibition of CD8$^+$ T-cells was observed by Mreg ($P < 0.05$) and by L-EV$_{Mreg}$ ($P < 0.01$ for 1.6×10^6 L-EV$_{Mreg}$/ml and 3.2×10^6 L-EV$_{Mreg}$/ml). PS was restricted to confined regions of the Mreg surface, while L-EV$_{Mreg}$ showed strong signals for PS in the exoplasmic leaflet. L-EV$_{Mreg}$ attenuate CD3/CD28-mediated activation of CD4$^+$ and CD8$^+$ T-cells. L-EV$_{Mreg}$ may have clinical relevance, particularly in the treatment of diseases associated with increased T-cell activity.

Key messages
- Mreg release large extracellular vesicles (L-EV$_{Mreg}$) with an average size of 7.5 μm
- L-EV$_{Mreg}$ exhibit phosphatidylserine positivity
- L-EV$_{Mreg}$ suppress CD4$^+$ and CD8$^+$ T-cells
- L-EV$_{Mreg}$ hold clinical potential in T-cell-related diseases

Keywords Macrophages · Large extracellular vesicles · T-cell activation · Phosphatidylserine

✉ Martin Albrecht
  martin.albrecht@uksh.de

[1] Department of Anesthesiology and Intensive Care Medicine, University Hospital of Schleswig-Holstein, Kiel, Germany

[2] Clinic of Cardiovascular Surgery, University Hospital of Schleswig-Holstein, Kiel, Germany

[3] Department of Pathology, University Hospital of Schleswig-Holstein, Kiel, Germany

[4] Clinic for Applied Cell Therapy, University Hospital of Schleswig-Holstein, Kiel, Germany

Introduction

Extracellular vesicles (EV) are small structures ranging from nano- to micrometer in size that are released by almost all cell types [1, 2]. EV contain lipids, proteins, and RNAs, making them an efficient way to transfer functional cargoes and signals between cells [1–4]. Growing evidence suggests that EV play a critical role in complex communication among different cell types [2, 5]. Interestingly, large

extracellular vesicles (L-EV), which range in diameter from 1 to 10 μm, have recently gained attention as potential sources of bioactive molecules and mediators of cell communication and angiogenesis [6, 7].

We have shown that human monocyte-derived regulatory macrophages (Mreg) contain and release pro-angiogenic proteins and produce large amounts of $L\text{-}EV_{Mreg}$ as part of their differentiation process [8]. These $L\text{-}EV_{Mreg}$ display an average size of 7.5 μm and an average volume of 0.2 pl. They carry distinct vesicular surface markers that characterize them as typical EV (LAMP-1, CD9, CD63, and CD81; based on MISEV guidelines 2018 [9]). In vitro, $L\text{-}EV_{Mreg}$ are able to promote wound healing and have a positive effect on several parameters of angiogenesis which suggests that they could bear therapeutic potential for the treatment of chronic wounds and ischemia-associated diseases such as peripheral arterial occlusive disease [8].

It has been described that macrophages, among their numerous other functions, are also able to communicate with and regulate immune cells [10, 11]. In this context, Mreg can inhibit the activation of immune cells and have been successfully employed as therapeutic approach in recipients of kidney transplant to minimize the burden of general immunosuppression [12]. However, whether $L\text{-}EV_{Mreg}$ are also able to regulate immune cells and which mechanisms are involved is still completely unclear. Here, we show that $L\text{-}EV_{Mreg}$ are generated during the in vitro differentiation of monocytes to Mreg. $L\text{-}EV_{Mreg}$ attenuate the CD3/CD28-induced activation of $CD4^+$ and $CD8^+$ T-cells and could therefore mediate immunomodulatory functions in vivo.

$L\text{-}EV_{Mreg}$ can be easily isolated from Mreg cultures by differential centrifugation and could be therapeutically valuable for many different clinical indications and diseases that are associated with a dysregulated immune response (i.e., increased T-cell activity).

Materials and methods

Mreg differentiation and isolation of L-EV$_{Mreg}$

The study was approved by the local Ethics Committee of the University Medical Center Schleswig-Holstein, Kiel, Germany (protocol identification: D519/18 and D518/13). Peripheral blood mononuclear cells (PBMC) were obtained from leukocyte reduction system (LRS) chambers provided by the Department of Transfusion Medicine (University Hospital of Schleswig-Holstein, Kiel, Germany). Monocytes were isolated and differentiated to Mreg as described earlier [8] and depicted in Fig. 1A. Briefly, PBMC were purified through a Ficoll-Paque PLUS gradient (GE Healthcare, Chicago, USA) and monocytes were recovered using a CD14 magnetic bead cell sorting system (Miltenyi, Bergisch

Gladbach, Germany) following the manufacturer's protocol. The isolated $CD14^+$ monocytes were cultivated in cell cultivation/differentiation bags (Miltenyi) at 0.83×10^6 cells/ml with RPMI 1640 medium containing GlutaMax (GIBCO, Billings, MT, USA) supplemented with 10% human AB-serum (Access Biological, Vista, CA, USA) and 2500 IU/ml human M-CSF (R&D Systems, Wiesbaden, Germany). After 6 days in culture, 500 IU/ml of human interferon (IFN) γ (R&D Systems, McKinley Place MN, USA) was added to the cultures and cells were incubated for additional 24 h. On day 7, Mreg were harvested and separated from culture medium by centrifugation (500xg for 10 min at room temperature; Fig. 1A). The pellets containing Mreg were resuspended in PBS and subjected to further analyses. The remaining culture supernatant containing EV was further centrifuged at 4000xg for 1 h at 4 °C and the $L\text{-}EV_{Mreg}$-containing pellet was resuspended in PBS and subjected to further analyses. Regarding Mreg and $L\text{-}EV_{Mreg}$ recovery at day 7, typically around 16×10^6 Mreg and 31×10^6 $L\text{-}EV_{Mreg}$ were obtained per 100-ml cultivation bag filled with 25ml culture medium.

Automated cell and vesicle analysis

Basic parameters such the number of particles (cells or vesicles) were evaluated using a MOXI cell counter (Orflo, Ketchum, ID, USA) which analyzes membrane surrounded structures within a size between 3 and 25 μm based on the Coulter principle (Fig. 1B, histogram).

In vitro T-cell activation assay

Employing the $CD14^+$ monocyte isolation methodology detailed in this context, the selection column allowed the passage of exclusively $CD14^-$ cells. These cells were harvested and employed as a source for T-cell activation assays (Fig. 1A). For the activation process, $CD14^-$ cells were pre-incubated with CD3/CD28 activation beads (Dynabeads Human T activation, Gibco, MA, USA) for 15 min, following the manufacturer's guidelines. Subsequently, $CD14^-$ cells (0.35×10^6/ml) were cultured either alone (activation control), in co-culture with Mreg (0.5×10^6/ml), or with varying concentrations of $L\text{-}EV_{Mreg}$ (0.8, 1.6, and 3.2×10^6/ml). The decision for the used concentrations of $L\text{-}EV_{Mreg}$ was based on the consideration that (i) the application of 0.5×10^6 Mreg/ml resulted in a statistically significant reduction of T-cell activation, and (ii) the $L\text{-}EV_{Mreg}$/Mreg ratio at the end of the differentiation period was 1.97 ± 0.64. After a co-incubation period of 3–5 days, supernatants containing non-adherent cells (including T-cells) were collected. The suspension was cleared of magnetic beads by positioning it near a magnetic field (MiniMACS™ separator, Miltenyi Biotec,
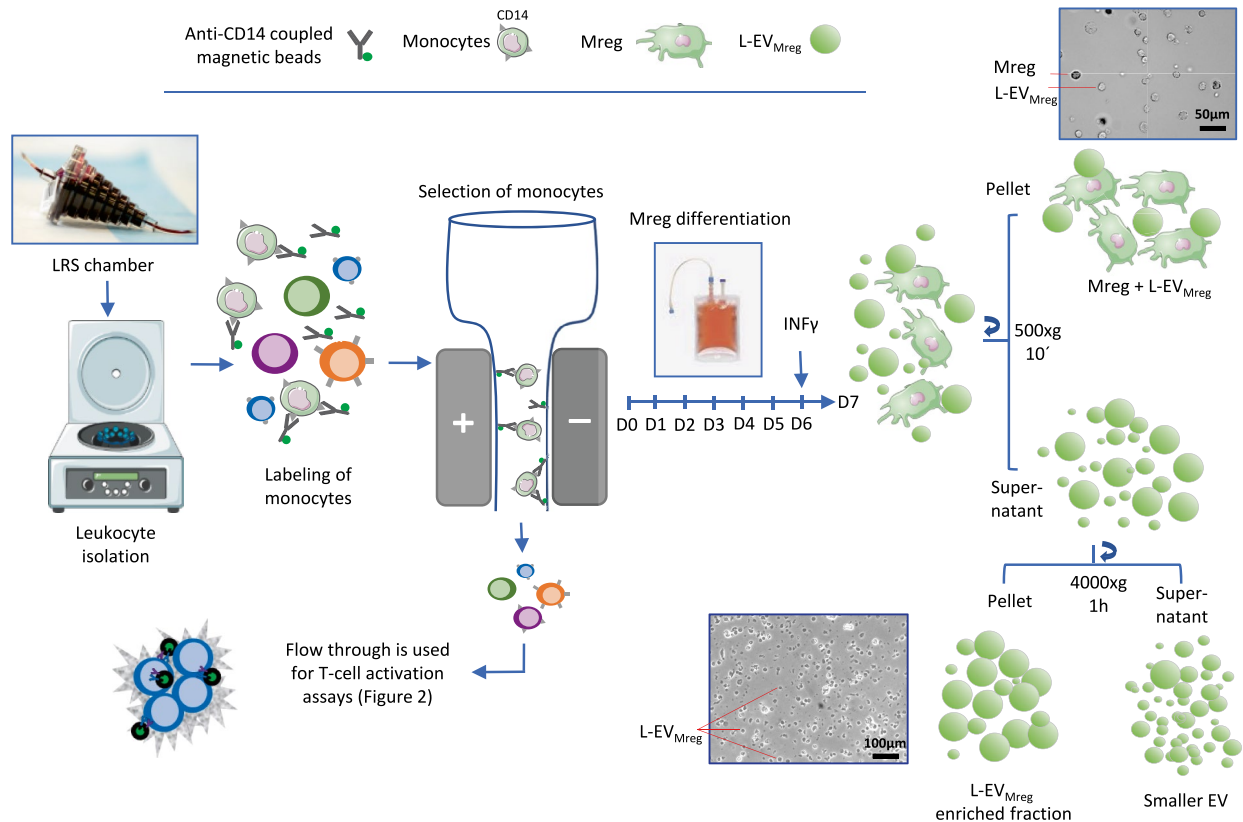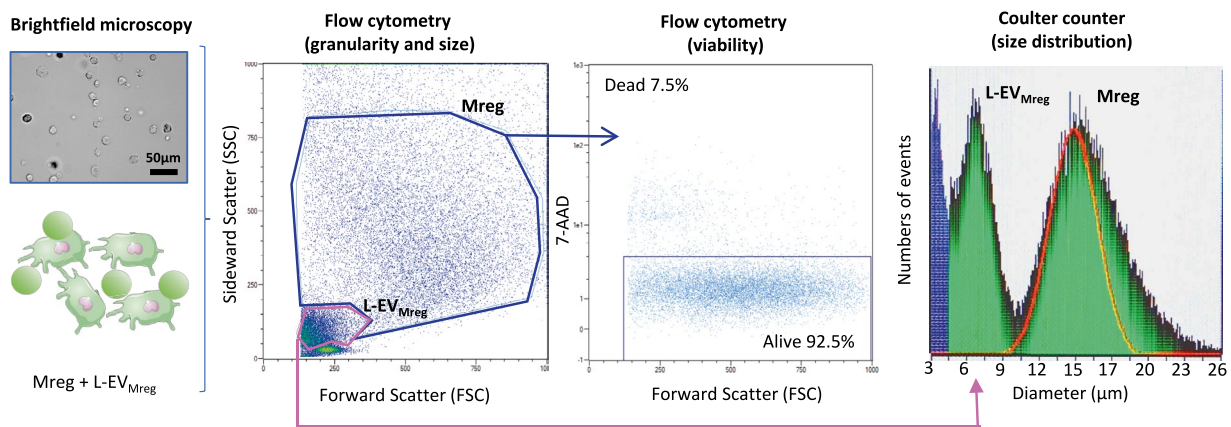
Fig. 1 Isolation and basic characterization of Mreg and L-EV$_{Mreg}$. **A** Schematic representation of the differentiation of Mreg from human monocytes and subsequent purification of L-EV$_{Mreg}$. **B** Results of the basic characterization of one representative Mreg and L-EV$_{Mreg}$ fraction by flow cytometry and Coulter counter–based analysis. Mreg and LEV$_{Mreg}$ can be distinguished as two distinct populations based on their granularity and size

Germany) for 5 min. Subsequently, the T-cells underwent flow cytometric analysis as described below (Fig. 2). For each T-cell activation assay, Mreg and L-EV$_{Mreg}$ from the same preparation/batch were used. Mreg or L-EV$_{Mreg}$ were not pooled.

Flow cytometry

Cell or vesicle surface markers were analyzed in each L-EV$_{Mreg}$/Mreg preparation by flow cytometry before cells and vesicles were used for further experiments.
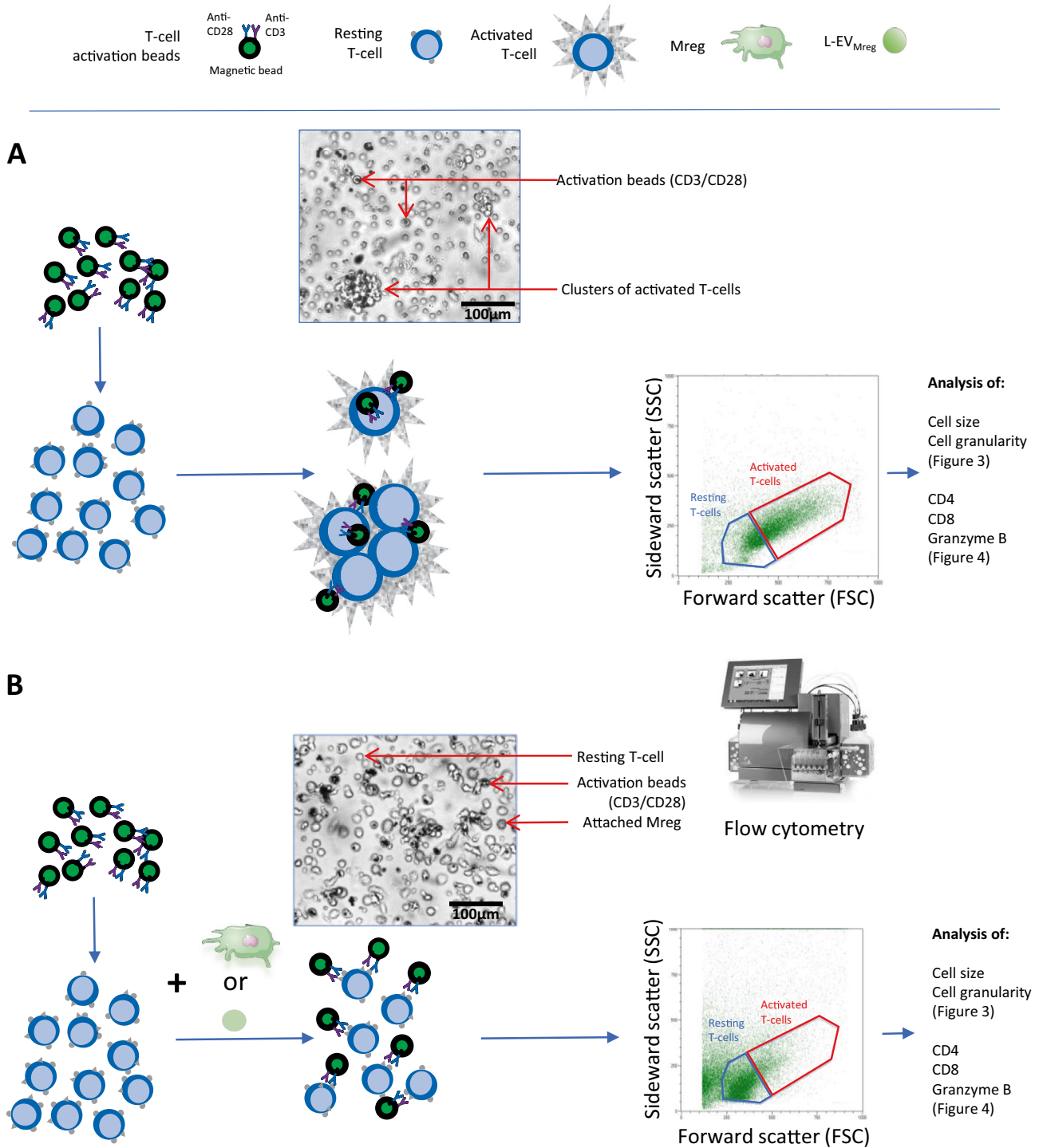
Fig. 2 Schematic illustration of CD3/CD28-induced T-cell activation. **A** Administration of CD3/CD28 Dynabeads and subsequent binding to the corresponding surface receptors on resting T-cells lead to their activation. Using brightfield microscopy, activated T-cells dominate as clusters of large cells and are also detectable in the FSC/SSC flow cytometry blots. **B** Addition of Mreg or increasing concentrations of L-EV$_{Mreg}$ to CD3/CD28-induced T-cells leads to inhibition of T-cell activation and lack of T-cell clustering

Standard markers that were examined are CD31, CD206, CD11c, CD86, CD14, CD16, CD103, CD38, CD45, LAMP-1, CD9, CD63, and CD81. For details, refer to our previous publication [8].

Flow cytometry was performed using the MACS Q10™ cytometer (Miltenyi Biotec, Germany). Fluorescein isothiocyanate (FITC)–conjugated specific antibodies including anti-CD4 and anti-mouse IgG1κ (both from BD Biosciences), phycoerythrin (PE)-conjugated anti-granzyme B, anti-mouse IgG1κ (both from Invitrogen), and allophycocyanin (APC)-conjugated anti-CD8 and anti-mouse IgG1κ (both from BD Biosciences) were used. To assess viability, 7-AAD (BD Biosciences) staining was used.

Cells were incubated with anti-CD4 and anti-CD8 antibodies or their respective isotype controls for 30 min at 4 °C. For analyses of intracellular granzyme B, cells were fixed, permeabilized with eBioscience Fixation/Permeabilization Concentrate (Invitrogen, USA), and incubated with granzyme B or the isotype control antibodies for 20 min at 4 °C. The gating strategy consisted of selecting the respective singlet population on a FSC-A/FSC-H plot, choosing the T-cell population based on size and granularity (FSC/SSC profile), and evaluating the respective target protein taking into account the isotype control signal of 7-AAD-negative (living) cells.

To evaluate the exposure of PS on the outer cell membrane by flow cytometry, an annexin V-FITC kit (Miltenyi Biotec, Germany) was employed following the manufacturer's instructions. Briefly, freshly isolated cells were incubated for 20 min with annexin V buffer and washed twice in the same buffer, and the final pellet was separated into four groups to incubate the cells (i) without any fluorochrome, (ii) with annexin V, (iii) with propidium iodide (PI), or (iv) with annexin V and PI. Annexin V was added and incubated for 20 min, while PI was added shortly before performing flow cytometry scans. Co-staining of cells with PI and annexin V was considered indicative of dead cells.

Fluorescence microscopy

For the visualization of PS in the outer cell/vesicle membrane, L-EV$_{Mreg}$-containing Mreg pellets were resuspended in a buffer consisting of 10 mM HEPES and 145 mM NaCl. The resuspended Mreg and L-EV$_{Mreg}$ were supplemented with 10 µM of PSVue480 (Molecular Targeting Technologies, West Chester, PA, USA) and 0.2 ng/ml of Hoechst33342 for nuclei staining. The mixture was then kept in the dark at 37 °C for 15 min before being centrifuged at 500xg for 5 min. The resulting pellets were then resuspended in HEPES buffer. A small quantity of the resuspended Mreg and L-EV$_{Mreg}$ was placed on a glass slide, covered with a glass coverslip, and immediately examined. The analysis was carried out using a Leica DM2000 LED fluorescent microscope equipped with DAPI, L5, and rhodamine filter cubes; a HC

PL FLUOTAR × 40/0.80 objective; and a Leica DFC7000 T fluorescence camera, using the Image Overlay software.

Statistics

All experiments were carried out with cells and L-EV$_{Mreg}$ derived from at least 5 healthy donors. The statistics software GraphPad Prism 5.01 for windows (GraphPad Software, San Diego, USA) was used to compare groups. All data were tested for normality using the Kolmogorov-Smirnov test. In cases normality was not obtained, the data were transformed (arcsin of square root of x) and analyzed using one-way ANOVA with Tukey test. A P-value < 0.05 was considered significant. All values are expressed as mean $\pm$ standard error mean (SEM).

Results

Basic characteristics of Mreg and L-EV$_{Mreg}$

The present study involves the characterization of monocyte-derived Mreg and L-EV$_{Mreg}$ obtained after 7 days of differentiation. Mreg recovery rate at harvest and viability were $71.83 \pm 5.91\%$ and $83.54 \pm 4.12\%$, respectively (data not shown). Visually, Mreg did not exhibit any signs of apoptosis such as blebbing or shrinkage and showed a typical morphology upon attachment to the culture well (Fig. 1A). Flow cytometry data revealed Mreg as highly viable granulated cell population, whereas L-EV$_{Mreg}$ dominated as a defined, less granulated population lacking nuclei (Figs. 1B and 4). Using the Coulter principle–based MOXI cell counter, the presence of two distinct populations, one of 7.47 ± 0.75µm corresponding to L-EV$_{Mreg}$ and the other of 13.73 ± 1.33µm corresponding to Mreg, could be confirmed (Fig. 1B). L-EV$_{Mreg}$ are only present in Mreg cultures; the culture medium as well as the added human AB serum is devoid of L-EV (data not shown). A characterization of Mreg and L-EV$_{Mreg}$ following the MISEV criteria [9] has been published by our group recently [8].

Effects of Mreg and L-EV$_{Mreg}$ on CD3/CD28-induced T-cell activation

T-cells can be activated in vitro through the simultaneous binding of CD3 and CD28 to the corresponding receptors on the T-cell surface which is achieved by the addition of CD3/CD28 coated beads to the respective lymphocyte preparations [13]. Activated T-cells are easily identified in culture by an increase in cell size and granularity and the presence of cell accumulations. While clusters of activated T-cells are already visible using conventional brightfield microscopy, the increase in cell size and granularity can be evaluated

by flow cytometry as a shift of the cell population toward higher FSC and SSC values. Using the described experimental setup (Fig. 2), we have analyzed the influence of Mreg and L-EV$_{Mreg}$ on T-cell activation.

In a first step, T-cell activation was estimated based on an increase in cell size (FSC in flow cytometry) and cell granularity (SSC in flow cytometry). Addition of Mreg resulted in a significant reduction in the number of activated T-cells compared to the control (CD3/CD28 activated T-cell control, 100%; Mreg, 42.42 ± 5.99%; $P < 0.0001$; Fig. 3). The addition of L-EV$_{Mreg}$ resulted in a dose-dependent inhibition of T-cell activation (CD3/CD28 activated T-cell control, 100%; 0.8×10^6 L-EV$_{Mreg}$/ml, 92.17 ± 3.29%, $P > 0.05$; 1.6×10^6 L-EV$_{Mreg}$/ml, 84.00 ± 3.53%, $P < 0.05$; 3.2×10^6 L-EV$_{Mreg}$/ml, 72.81 ± 4.80%, $P < 0.05$; Fig. 3).

Since activated T-cells express large amounts of intracellular granzyme B [14, 15], this enzyme was used as additional reliable intracellular marker to quantify the number of activated T-cells.

Our results show that the addition of Mreg causes a significant reduction in the number of activated T-cells compared to the control (CD3/CD28 activated T-cell control, 100%; Mreg, 17.29 ± 3.35%; $P < 0.001$; Fig. 4A). The addition of L-EV$_{Mreg}$ resulted in a dose-dependent inhibition of T-cell activation, although a statistically significant effect could only be achieved with the highest

concentration of L-EV$_{Mreg}$ (CD3/CD28 activated T-cell control, 100%; 0.8×10^6 L-EV$_{Mreg}$/ml, 88.41 ± 9.38%, $P > 0.05$; 1.6×10^6 L-EV$_{Mreg}$/ml, 72.95 ± 17.51%, $P > 0.05$; 3.2×10^6 L-EV$_{Mreg}$/ml, 57.48 ± 13.30%, $P < 0.05$; Fig. 4A).

Additional stratification of T-cells into CD4$^+$ helper T-cells and CD8$^+$ cytotoxic T-cells showed that both Mreg and L-EV$_{Mreg}$ were able to inhibit CD3/CD28-induced activation of both T-cell subpopulations: CD4$^+$ T-cells: CD3/CD28 activated CD4$^+$ T-cell control, 58.42 ± 6.58% (granzyme B–positive cells); Mreg, 40.68 ± 4.19%, $P < 0.01$; 0.8×10^6 L-EV$_{Mreg}$/ml, 50.61 ± 7.72%, $P > 0.05$; 1.6×10^6 L-EV$_{Mreg}$/ml, 43.33 ± 11.18%, $P < 0.05$; 3.2×10^6 L-EV$_{Mreg}$/ml, 37.93 ± 6.78%, $P < 0.01$; Fig. 4B. CD8$^+$ T-cells: CD3/CD28 activated CD8$^+$ T-cell control, 26.89 ± 5.51% (granzyme B–positive cells); Mreg, 20.43 ± 3.48%, $P < 0.05$; 0.8×10^6 L-EV$_{Mreg}$/ml, 22.71 ± 4.77%, $P > 0.05$; 1.6×10^6 L-EV$_{Mreg}$/ml, 18.61 ± 5.15%, $P < 0.01$; 3.2×10^6 L-EV$_{Mreg}$/ml, 17.16 ± 3.37%, $P < 0.01$; Fig. 4C.

Another marker for the assessment of T-cell activation is CD25 which is upregulated on the surface of activated T-cells and serves as a high-affinity receptor for interleukin-2 (IL-2), a key cytokine involved in T-cell proliferation and survival [16]. In addition to the granzyme B evaluation, quantification of the number of CD25-positive T-cells also confirmed the above described effects of T-cell inhibition by Mreg and L-EV$_{Mreg}$ (data not shown).

Fig. 3 Effects of Mreg and L-EV$_{Mreg}$ on the T-cell activation (cell size and cell granularity). Relative number of activated T-cells. A representative flow cytometry dot plot is shown below the respective columns. *$P < 0.05$; ****$P < 0.0001$ vs. activated T-cells (group: T-cells + CD3/CD28 beads)
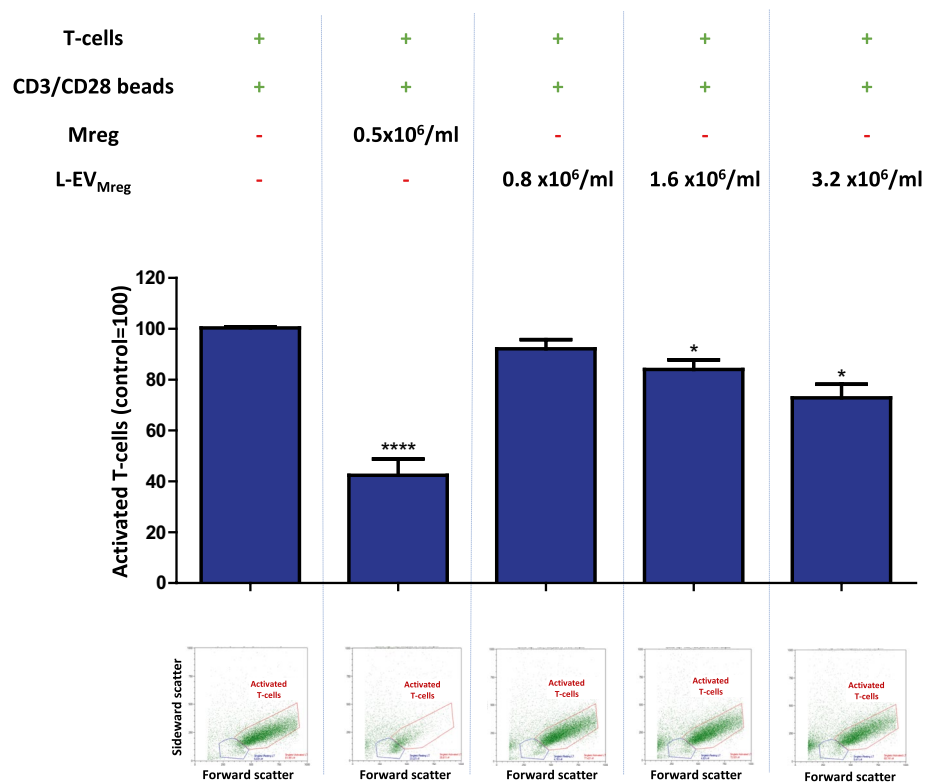
Fig. 4 Effects of Mreg and L-EV$_{Mreg}$ on the T-cell activation (intracellular granzyme B). **A** Relative number of activated T-cells. **B** Activated CD4$^+$ T-cells. **C** Activated CD8$^+$ T-cells. A representative flow cytometry dot plot is shown below the respective columns in **B** and **C**. *$P < 0.05$; **$P < 0.01$; ***$P < 0.001$ vs. activated T-cells (group: T-cells + CD3/CD28 beads)
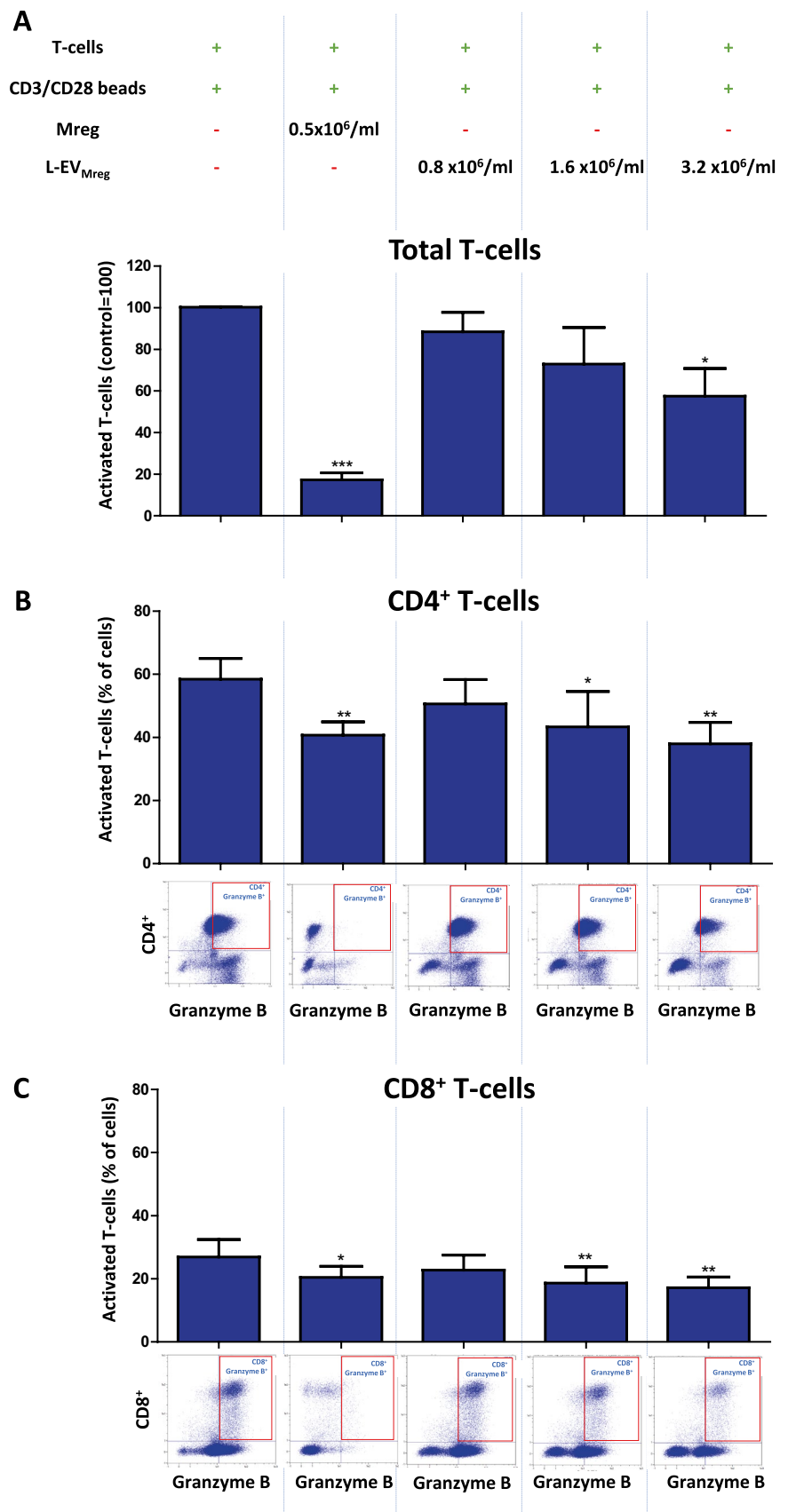
Phosphatidylserine exposure on the membrane of Mreg and L-EV$_{Mreg}$

As the exposure of phosphatidylserine (PS) by non-apoptotic cells has been recently recognized as an immunomodulatory mechanism [17] and PS is present in the cell membrane of non-apoptotic macrophages [18], we decided to analyze whether PS is also detectable in the outer lipid bilayer of Mreg and L-EV$_{Mreg}$. Nuclear staining for viable cells and PS staining were performed on Mreg and L-EV$_{Mreg}$. The results show that Mreg are either negative for PS or that PS is restricted to a confined region of the cell surface. In contrast to Mreg, L-EV$_{Mreg}$ lack nuclei and show strong signals for PS on the entire surface (Fig. 5A–C). Extended analysis of the vesicular fraction by cytometry confirmed the fluorescence microscopy findings defining L-EV$_{Mreg}$ as PS-positive vesicular structures devoid of nuclei.

Discussion

Eukaryotic cells release extracellular vesicles (EV) into their microenvironment, which can vary in size and cargo composition [1, 2, 19]. EV transport a plethora of diverse biological molecules including lipids, carbohydrates, proteins, and RNAs, and their characteristics may vary depending on the conditions they are exposed to, allowing them to effectively transmit functional content and signals between cells [1, 2, 5, 20].

Macrophages are a type of white blood cell that play diverse roles in the immune response, including phagocytosis, antigen presentation, and regulation of inflammation. They can be polarized into different subsets, such as M1 and M2, which exhibit distinct functional and phenotypic characteristics [21, 22]. Macrophage-derived EV [23] have been found to play a role in numerous physiological and pathological pathways [24, 25] and to modulate immune responses [25–27].

Regulatory macrophages (Mreg), which in particular possess characteristics of anti-inflammatory M2 macrophages, can be generated from peripheral blood monocytes under defined growth factor-induced culture conditions [28–30]. Mreg secrete pro-angiogenic factors as well as various cytokines and have already been used in cell therapy–based trials to reduce organ rejection after kidney transplantation [12, 30]. In this context, intravenously applied Mreg minimized the burden of general immunosuppression after organ transplantation [12] and the underlying mechanisms may involve a Mreg-mediated inhibition of immune cell activation [10].

In our recent work, we have shown that monocyte-derived Mreg also secrete large EV (L-EV$_{Mreg}$), with an average diameter of 7.5 μm and an average volume of 0.22 pl, which contain pro-angiogenic molecules and induce angiogenesis and wound healing in vitro [8]. Here, we demonstrate for

the first time that L-EV$_{Mreg}$ are also able to attenuate CD3/CD28-induced activation of CD4$^+$ and CD8$^+$ T-cells.

T-cells play a crucial role in the immune system function by recognizing and responding to foreign antigens. Upon activation, they proliferate and differentiate into effector T-cells that coordinate an immune response against the pathogen [31]. Effector T-cells can be divided into helper and cytotoxic T-cells [32, 33]. Helper T-cells also known as CD4$^+$ T-cells recognize and bind to antigen-presenting cells and provide help to other immune cells, such as B-cells and macrophages, to mount an effective immune response. They secrete cytokines that activate and coordinate the immune response against the pathogen [34, 35]. In contrast, cytotoxic T-cells, also known as CD8$^+$ T-cells, recognize and kill infected or cancerous cells through the release of cytotoxic molecules. They play a crucial role in the elimination of intracellular pathogens and tumor cells [36]. Dysregulation of T-cell function can lead to various immune-related disorders, including autoimmune diseases and cancer [37–39].

Utilizing cytometric analyses, the current investigation revealed that both Mreg and L-EV$_{Mreg}$ possess the ability to attenuate T-cell activation induced by CD3/CD28 stimulation. The suppressive potential of Mreg was found to be considerably greater compared to L-EV$_{Mreg}$; however, the latter still exhibited a statistically significant level of T-cell inhibition, particularly at the highest concentration of 3.2×10^6 L-EV$_{Mreg}$/ml employed. Despite the inferiority of L-EV$_{Mreg}$ in terms of T-cell inhibition when compared to Mreg, L-EV$_{Mreg}$ present numerous advantages for potential clinical applications: one major advantage of L-EV$_{Mreg}$ is their lack of a cellular nucleus and inability to replicate. Consequently, L-EV$_{Mreg}$ do not possess characteristics of living organisms, which reduces the likelihood of side effects that are commonly associated with the administration of autologous or allogeneic cells in a clinical context. Moreover, large quantities of L-EV$_{Mreg}$ can be obtained from Mreg cultures as they are continually produced by Mreg and storage and handling of L-EV$_{Mreg}$ are also considerably more convenient than those of vital Mreg cells. Finally, since L-EV$_{Mreg}$ do not fall under the classification of Advanced Therapy Medicinal Products (ATMPs), they are exempt from the corresponding regulatory restrictions. This enables a faster and more convenient transition of a possible L-EV$_{Mreg}$ treatment into clinical applications.

Regarding the eukaryotic lipid bilayer cell membrane, it is widely accepted that apoptosis triggers the exposure of PS on the outer membrane surface [40]. However, this distribution pattern of PS can also be observed in non-apoptotic cells [41] and it was shown that PS expressed on the surface of human exosomes is linked to T-cell immunosuppression [40, 42]. Therefore, it could be proposed that the exposure of PS in the exoplasmic leaflet of Mreg and L-EV$_{Mreg}$ described in the present work may be involved in the

Fig. 5 Phosphatidylserine exposure on the membrane of Mreg and L-EV$_{Mreg}$. **A** Cells and vesicles were stained with Hoechst33342 (violet) and PSVue480 (green) to label DNA and PS, respectively. Signals were merged on the brightfield background to distinguish morphological features. Yellow arrows show L-EV$_{Mreg}$. Bar denotes 50 μm. **B** Left: magnified views of two selected areas from **A**. Right: same area as on the left showing only the nuclei staining. Yellow arrows denote L-EV$_{Mreg}$. Note that L-EV$_{Mreg}$ lack nuclei and are positive for PS, while Mreg contain nuclei and are either negative for PS or reveal PS to be restricted to only a confined region of the cell surface. Bar denotes 20 μm. **C** Typical PS staining of a Mreg cell and one L-EV$_{Mreg}$. Yellow arrows denote L-EV$_{Mreg}$. Bar denotes 15 μm. **D** Left: Flow cytometry and gating (red box) of L-EV$_{Mreg}$. Right: Gated L-EV$_{Mreg}$ are positive for PS (annexin V staining) and negative for nucleic acids (propidium iodide staining)
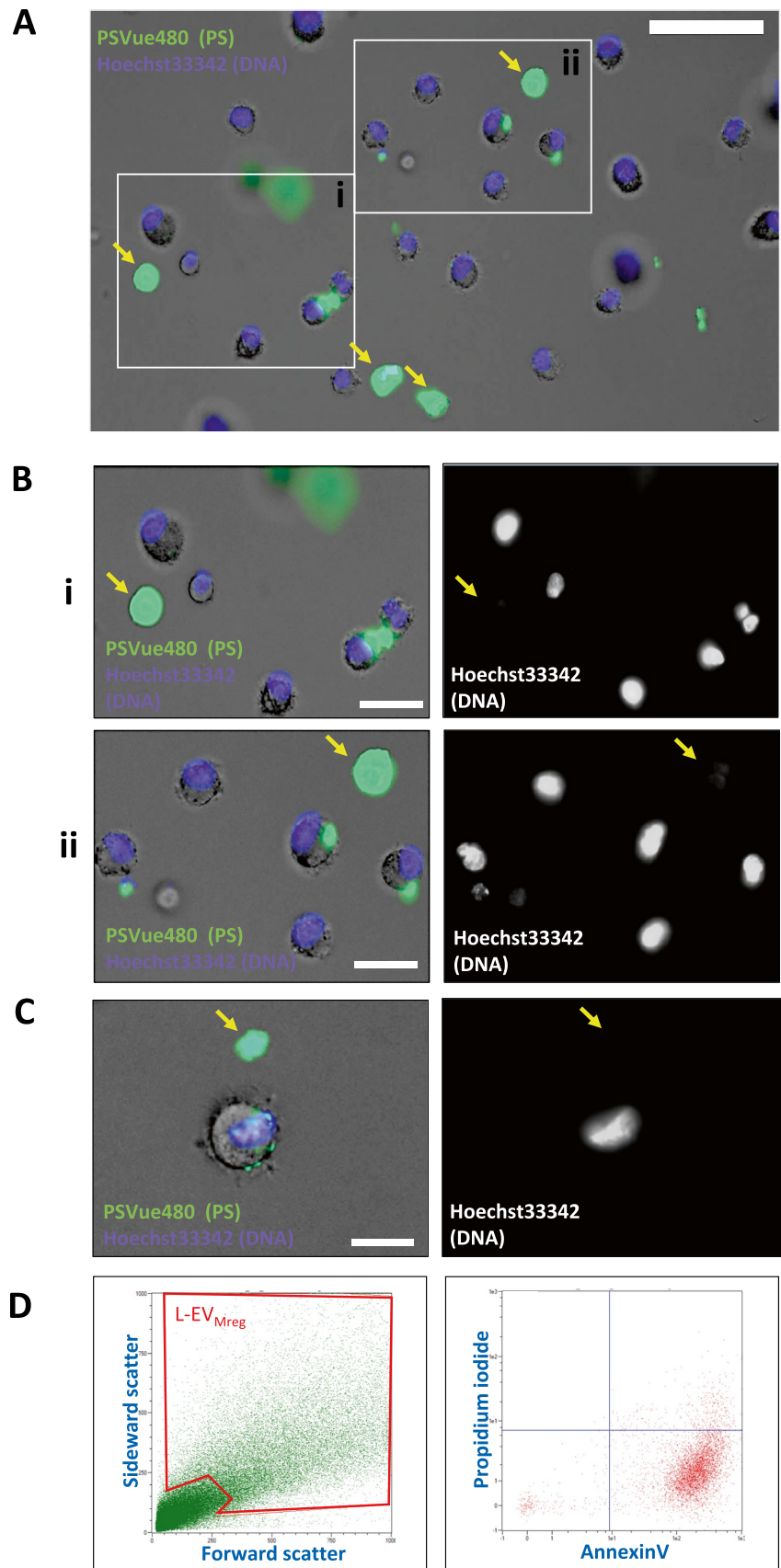
Mreg- and L-EV$_{Mreg}$-mediated attenuation of T-cell activation. Also, the PD-1/PD-L1 system, which plays an important role in regulating several components of the immune system [43–45], might be involved in T-cell regulation. Preliminary findings of our group showed that $82.6 \pm 3.8\%$ of Mreg and $22.0 \pm 6.1\%$ of L-EV$_{Mreg}$ are positive for PD-L1, the ligand for PD-1 which is expressed on the surface of T-cells [43, 46]. Although the above-mentioned potential mechanisms of T-cell inhibition by L-EV$_{Mreg}$ are scientifically of interest, they are of only secondary importance for the potential clinical application of L-EV$_{Mreg}$ and were not the main objective of our present work.

It should be noted that despite intensive characterization of L-EV$_{Mreg}$, their categorization into the different classes of EV is not fully established at this stage. However, there are several similarities between exophers and L-EV$_{Mreg}$ [47]. Exophers are several micrometers in size and have been demonstrated to detach from cells within a matter of hours [48]. Unfortunately, we are unable to investigate this characteristic trait of exophers in the context of L-EV$_{Mreg}$. Throughout the differentiation phase, Mreg remain within the culture bags inside the incubator, rendering them inaccessible to morphological analyses. Furthermore, even the simple act of transferring the bags from the incubator to the microscope is likely to dissolve any potential connection between the exophers and their parent cells. However, exophers typically possess a lipid bilayer and exhibit phosphatidylserine on their surface, thereby sharing certain characteristics with the L-EV$_{Mreg}$ described in our study [48].

In conclusion, the present study has revealed the novel finding that PS positive L-EV$_{Mreg}$ can suppress both CD4$^+$ and CD8$^+$ T-cells, suggesting the potential clinical use of L-EV$_{Mreg}$ in various diseases associated with increased T-cell activity, including multiple sclerosis, rheumatoid arthritis, type 1 diabetes, allergic reactions, and transplant rejection.

Declarations

Ethics approval and consent to participate The study was approved by the local Ethics Committee of the University Medical Center Schleswig-Holstein, Kiel, Germany (protocol identification: D519/18 and D518/13).

Consent for publication Not applicable.

Competing interests The authors (MA, KZ, FF, RB) are involved in a pending patent (European Patent Office, Nr. 23153832.3 Mreg-derived vesicles). All other authors declare no competing interests.

References

1. Teng F, Fussenegger M (2020) Shedding light on extracellular vesicle biogenesis and bioengineering. Adv Sci (Weinh) 8:2003505. https://doi.org/10.1002/advs.202003505

2. Kang T, Atukorala I, Mathivanan S (2021) Biogenesis of extracellular vesicles. Subcell Biochem 97:19–43. https://doi.org/10.1007/978-3-030-67171-6_2

3. Chang X, Fang L, Bai J, Wang Z (2020) Characteristics and changes of DNA in extracellular vesicles. DNA Cell Biol 39:1486–1493. https://doi.org/10.1089/dna.2019.5005

4. Heydari Z, Peshkova M, Gonen ZB, Coretchi I, Eken A, Yay AH, Dogan ME, Gokce N, Akalin H, Kosheleva N et al (2023) EVs vs. EVs: MSCs and Tregs as a source of invisible possibilities. J Mol Med (Berl) 101:51–63. https://doi.org/10.1007/s00109-022-02276-2

5. Weng Q, Wang Y, Xie Y, Yu X, Zhang S, Ge J, Li Z, Ye G, Guo J (2022) Extracellular vesicles-associated tRNA-derived fragments (tRFs): biogenesis, biological functions, and their role as potential biomarkers in human diseases. J Mol Med (Berl) 100:679–695. https://doi.org/10.1007/s00109-022-02189-0

6. Todorova D, Simoncini S, Lacroix R, Sabatier F, Dignat-George F (2017) Extracellular vesicles in angiogenesis. Circ Res 120:1658–1673. https://doi.org/10.1161/CIRCRESAHA.117.309681

7. Slomka A, Urban SK, Lukacs-Kornek V, Zekanowska E, Kornek M (2018) Large extracellular vesicles: have we found the holy grail of inflammation? Front Immunol 9:2723. https://doi.org/10.3389/fimmu.2018.02723

8. Albrecht M, Hummitzsch L, Rusch R, Hess K, Steinfath M, Cremer J, Lichte F, Fandrich F, Berndt R, Zitta K (2023) Characterization of large extracellular vesicles (L-EV) derived from human regulatory macrophages (Mreg): novel mediators in wound healing and angiogenesis? J Transl Med 21:61. https://doi.org/10.1186/s12967-023-03900-6

9. Thery C, Witwer KW, Aikawa E, Alcaraz MJ, Anderson JD, Andriantsitohaina R, Antoniou A, Arab T, Archer F, Atkin-Smith GK et al (2018) Minimal information for studies of extracellular vesicles 2018 (MISEV2018): a position statement of the International Society for Extracellular Vesicles and update of the

MISEV2014 guidelines. J Extracell Vesicles 7:1535750. https://doi.org/10.1080/20013078.2018.1535750

10. Riquelme P, Govert F, Geissler EK, Fandrich F, Hutchinson JA (2009) Human transplant acceptance-inducing cells suppress mitogen-stimulated T cell proliferation. Transpl Immunol 21:162–165. https://doi.org/10.1016/j.trim.2009.03.004

11. Salminen A (2021) Immunosuppressive network promotes immunosenescence associated with aging and chronic inflammatory conditions. J Mol Med (Berl) 99:1553–1569. https://doi.org/10.1007/s00109-021-02123-w

12. Sawitzki B, Harden PN, Reinke P, Moreau A, Hutchinson JA, Game DS, Tang Q, Guinan EC, Battaglia M, Burlingham WJ et al (2020) Regulatory cell therapy in kidney transplantation (The ONE Study): a harmonised design and analysis of seven non-randomised, single-arm, phase 1/2A trials. Lancet 395:1627–1639. https://doi.org/10.1016/S0140-6736(20)30167-7

13. Tumaini B, Lee DW, Lin T, Castiello L, Stroncek DF, Mackall C, Wayne A, Sabatino M (2013) Simplified process for the production of anti-CD19-CAR-engineered T cells. Cytotherapy 15:1406–1415. https://doi.org/10.1016/j.jcyt.2013.06.003

14. Mellor-Heineke S, Villanueva J, Jordan MB, Marsh R, Zhang K, Bleesing JJ, Filipovich AH, Risma KA (2013) Elevated granzyme B in cytotoxic lymphocytes is a signature of immune activation in hemophagocytic lymphohistiocytosis. Front Immunol 4:72. https://doi.org/10.3389/fimmu.2013.00072

15. Grossman WJ, Verbsky JW, Tollefsen BL, Kemper C, Atkinson JP, Ley TJ (2004) Differential expression of granzymes A and B in human cytotoxic lymphocyte subsets and T regulatory cells. Blood 104:2840–2848. https://doi.org/10.1182/blood-2004-03-0859

16. Cantrell D (2015) Signaling in lymphocyte activation. Cold Spring Harb Perspect Biol 7. https://doi.org/10.1101/cshperspect.a018788

17. Shlomovitz I, Speir M, Gerlic M (2019) Flipping the dogma - phosphatidylserine in non-apoptotic cell death. Cell Commun Signal 17:139. https://doi.org/10.1186/s12964-019-0437-0

18. Callahan MK, Williamson P, Schlegel RA (2000) Surface expression of phosphatidylserine on macrophages is required for phagocytosis of apoptotic thymocytes. Cell Death Differ 7:645–653. https://doi.org/10.1038/sj.cdd.4400690

19. Abels ER, Breakefield XO (2016) Introduction to extracellular vesicles: biogenesis, RNA cargo selection, content, release, and uptake. Cell Mol Neurobiol 36:301–312. https://doi.org/10.1007/s10571-016-0366-z

20. Akers JC, Gonda D, Kim R, Carter BS, Chen CC (2013) Biogenesis of extracellular vesicles (EV): exosomes, microvesicles, retrovirus-like vesicles, and apoptotic bodies. J Neurooncol 113:1–11. https://doi.org/10.1007/s11060-013-1084-8

21. Murray PJ, Wynn TA (2011) Protective and pathogenic functions of macrophage subsets. Nat Rev Immunol 11:723–737. https://doi.org/10.1038/nri3073

22. Mosser DM, Edwards JP (2008) Exploring the full spectrum of macrophage activation. Nat Rev Immunol 8:958–969. https://doi.org/10.1038/nri2448

23. Dechantsreiter S, Ambrose AR, Worboys JD, Lim JME, Liu S, Shah R, Montero MA, Quinn AM, Hussell T, Tannahill GM et al (2022) Heterogeneity in extracellular vesicle secretion by single human macrophages revealed by super-resolution microscopy. J Extracell Vesicles 11:e12215. https://doi.org/10.1002/jev2.12215

24. Wang Y, Zhao M, Liu S, Guo J, Lu Y, Cheng J, Liu J (2020) Macrophage-derived extracellular vesicles: diverse mediators of pathology and therapeutics in multiple diseases. Cell Death Dis 11:924. https://doi.org/10.1038/s41419-020-03127-z

25. Xing Y, Sun X, Dou Y, Wang M, Zhao Y, Yang Q, Zhao Y (2021) The immuno-modulation effect of macrophage-derived extracellular vesicles in chronic inflammatory diseases. Front Immunol 12:785728. https://doi.org/10.3389/fimmu.2021.785728

26. Morrison TJ, Jackson MV, Cunningham EK, Kissenpfennig A, McAuley DF, O'Kane CM, Krasnodembskaya AD (2017) Mesenchymal stromal cells modulate macrophages in clinically relevant lung injury models by extracellular vesicle mitochondrial transfer. Am J Respir Crit Care Med 196:1275–1286. https://doi.org/10.1164/rccm.201701-0170OC

27. Tang D, Cao F, Yan C, Fang K, Ma J, Gao L, Sun B, Wang G (2022) Extracellular vesicle/macrophage axis: potential targets for inflammatory disease intervention. Front Immunol 13:705472. https://doi.org/10.3389/fimmu.2022.705472

28. Gurvich OL, Puttonen KA, Bailey A, Kailaanmaki A, Skirdenko V, Sivonen M, Pietikainen S, Parker NR, Yla-Herttuala S, Kekarainen T (2020) Transcriptomics uncovers substantial variability associated with alterations in manufacturing processes of macrophage cell therapy products. Sci Rep 10:14049. https://doi.org/10.1038/s41598-020-70967-2

29. Hutchinson JA, Ahrens N, Geissler EK (2017) MITAP-compliant characterization of human regulatory macrophages. Transpl Int 30:765–775. https://doi.org/10.1111/tri.12988

30. Hummitzsch L, Zitta K, Rusch R, Cremer J, Steinfath M, Gross J, Fandrich F, Berndt R, Albrecht M (2019) Characterization of the angiogenic potential of human regulatory macrophages (Mreg) after ischemia/reperfusion injury in vitro. Stem Cells Int 2019:3725863. https://doi.org/10.1155/2019/3725863

31. Krogsgaard M, Davis MM (2005) How T cells 'see' antigen. Nat Immunol 6:239–245. https://doi.org/10.1038/ni1173

32. Harty JT, Badovinac VP (2008) Shaping and reshaping CD8+ T-cell memory. Nat Rev Immunol 8:107–119. https://doi.org/10.1038/nri2251

33. Williams MA, Bevan MJ (2007) Effector and memory CTL differentiation. Annu Rev Immunol 25:171–192. https://doi.org/10.1146/annurev.immunol.25.022106.141548

34. Wan YY, Flavell RA (2007) 'Yin-Yang' functions of transforming growth factor-beta and T regulatory cells in immune regulation. Immunol Rev 220:199–213. https://doi.org/10.1111/j.1600-065X.2007.00565.x

35. Vignali DA, Collison LW, Workman CJ (2008) How regulatory T cells work. Nat Rev Immunol 8:523–532. https://doi.org/10.1038/nri2343

36. Halle S, Halle O, Forster R (2017) Mechanisms and dynamics of T cell-mediated cytotoxicity in vivo. Trends Immunol 38:432–443. https://doi.org/10.1016/j.it.2017.04.002

37. Sospedra M, Martin R (2005) Immunology of multiple sclerosis. Annu Rev Immunol 23:683–747. https://doi.org/10.1146/annurev.immunol.23.021704.115707

38. Atkinson MA, Eisenbarth GS, Michels AW (2014) Type 1 diabetes. Lancet 383:69–82. https://doi.org/10.1016/S0140-6736(13)60591-7

39. Wherry EJ, Kurachi M (2015) Molecular and cellular insights into T cell exhaustion. Nat Rev Immunol 15:486–499. https://doi.org/10.1038/nri3862

40. Bhatta M, Shenoy GN, Loyall JL, Gray BD, Bapardekar M, Conway A, Minderman H, Kelleher RJ, Jr., Carreno BM, Linette G et al (2021) Novel phosphatidylserine-binding molecule enhances antitumor T-cell responses by targeting immunosuppressive exosomes in human tumor microenvironments. J Immunother Cancer 9. https://doi.org/10.1136/jitc-2021-003148

41. Thery C, Ostrowski M, Segura E (2009) Membrane vesicles as conveyors of immune responses. Nat Rev Immunol 9:581–593. https://doi.org/10.1038/nri2567

42. Zhao X, Yuan C, Wangmo D, Subramanian S (2021) Tumor-secreted extracellular vesicles regulate T-cell costimulation and can be manipulated to induce tumor-specific T-cell responses. Gastroenterology 161:560–574 e511. https://doi.org/10.1053/j.gastro.2021.04.036

43. Sharpe AH, Pauken KE (2018) The diverse functions of the PD1 inhibitory pathway. Nat Rev Immunol 18:153–167. https://doi.org/10.1038/nri.2017.108

44. Roux C, Jafari SM, Shinde R, Duncan G, Cescon DW, Silvester J, Chu MF, Hodgson K, Berger T, Wakeham A et al (2019) Reactive oxygen species modulate macrophage immunosuppressive phenotype through the up-regulation of PD-L1. Proc Natl Acad Sci U S A 116:4326–4335. https://doi.org/10.1073/pnas.1819473116

45. Ai L, Chen J, Yan H, He Q, Luo P, Xu Z, Yang X (2020) Research status and outlook of PD-1/PD-L1 inhibitors for cancer therapy. Drug Des Devel Ther 14:3625–3649. https://doi.org/10.2147/DDDT.S267433

46. Konkel JE, Frommer F, Leech MD, Yagita H, Waisman A, Anderton SM (2010) PD-1 signalling in CD4(+) T cells restrains their clonal expansion to an immunogenic stimulus, but is not critically required for peptide-induced tolerance. Immunology 130:92–102. https://doi.org/10.1111/j.1365-2567.2009.03216.x

47. Arnold ML, Cooper J, Grant BD, Driscoll M (2020) Quantitative approaches for scoring in vivo neuronal aggregate and organelle extrusion in large exopher vesicles in C. elegans. J Vis Exp. https://doi.org/10.3791/61368

48. Jeppesen DK, Zhang Q, Franklin JL, Coffey RJ (2023) Extracellular vesicles and nanoparticles: emerging complexities. Trends Cell Biol 33:667–681. https://doi.org/10.1016/j.tcb.2023.01.002

Publisher's Note Springer Nature remains neutral with regard to jurisdictional claims in published maps and institutional affiliations.